J. Synchrotron Rad. (1998). **5**, 293–298

Spectroscopic Techniques using Synchrotron Radiation and Free-Electron and Conventional Lasers

A. Tadjeddine,[a]* A. Peremans,[a,b] A. Le Rille,[a] W. Q. Zheng,[a] J. M. Ortéga,[a] F. Glotin,[a] R. Prazeres,[a] M. Meyer,[a] J. Lacoursière,[c] L. Nahon,[a,d] M. Gisselbrecht,[a] P. Morin,[a,d] M. Larzillière,[c] M. Marsi,[e] A. Taleb-Ibrahimi,[a] M. E. Couprie,[a,d] T. Hara[f] and D. Garzella[d]

[a]LURE, Bâtiment 209D, Université Paris-Sud, 91405 Orsay, France, [b]LASMOS, Facultés Universitaires Notre-Dame de la Paix, B-5àà à Namur, Belgium, [c]LPAM, Département de Physique, Université Laval, Quèbec, Canada G1K7P4, [d]CEA, DRECAM, SPAM, CEN Saclay, 91191 Gif-sur-Yvette, France, [e]Sincrotrone Trieste, Padriciamo 99, I-134012 Trieste, Italy, and [f]Spring-8, Hyogo 678-12, Japan. E-mail: tadjeddine@lure.u-psud.fr

(*Received 4 August 1997; accepted 3 December 1997*)

Considerable progress in the investigation of the electronic and vibrational properties of atoms, molecules, materials, surfaces and interfaces has been achieved by combining different photon sources of complementary characteristics. In this paper some experimental results obtained recently at LURE by using two synchronized sources, such as the IR free-electron laser (FEL) CLIO, the VUV storage ring FEL, synchrotron radiation and table lasers, are presented. Using CLIO synchronized with a YAG laser allows the investigation of the vibrational properties of adsorbed species by the non-linear optical technique of visible–IR sum (difference) frequency generation, as shown for the adsorption of hydrogen on platinum in the electrochemical environment. The second result reported here relates to the study of the intersubband stimulated emission in GaAs/GaAlAs quantum wells by pump-probe experiments using the two-colour configuration of CLIO. The combination of a mode-locked Ar^+ laser and synchrotron radiation has been used for investigations in a pump-probe arrangement of the ionization of Xe atoms *via* the resonant state Xe* $5p^5 5d\ [3/2]_1$. The final example is a time-resolved core-level spectroscopy study of photoexcited Si(111) 2×1 surfaces by using a combination of the naturally synchronized UV storage ring laser and synchrotron radiation.

Keywords: free-electron lasers; two-colour configurations; spectroscopy.

1. Introduction

The combination of photon sources of different and complementary characteristics represents a very powerful research technique for various scientific areas, such as solid-state physics, surface and interface science, electrochemistry and catalysis, and atomic and molecular spectroscopy. The aim of this paper is to illustrate, through some selected results recently obtained in our laboratory, the extraordinary opportunity brought about by this approach. The first example is the use of the linac-driven IR free-electron laser (FEL) CLIO (Collaboration pour un Laser Infrarouge à Orsay) synchronized with a YAG laser for investigation of the vibrational properties of interfacial species by visible–IR sum and difference frequency generation. We then present the application of the two-colour configuration of CLIO to the study of the optical gain associated with intersubband stimulated emission in optically pumped coupled quantum wells. The third example concerns atomic and molecular spectroscopy in the gas phase and describes a resonant two-photon ionization using an Ar^+ mode-locked laser synchronized with VUV pulses from the Super-ACO storage ring. The final example presents the application of a novel approach to two-photon spectroscopy, based on the combined use of the naturally synchronized storage ring FEL and synchrotron radiation of Super-ACO to the study of surface states and space charge dynamics on semiconductor surfaces and interfaces.

2. Vibrational spectroscopy of interfaces by visible–IR sum (SFG) and difference (DFG) frequency generation using the IR CLIO FEL

2.1. *CLIO FEL (Ortéga, 1996)*

The advantage of the FEL over a conventional laser is that it is broadly tunable and powerful at any wavelength. The gain medium of an FEL is a high-energy electron beam (several MeV) passing through a transverse magnetic field of an undulator. The interaction in the undulator of the emitted radiation with the electron beam

leads to light amplification. This effect, when operating within an optical cavity, is the principle of the free-electron laser.

The laser radiation is emitted by the FEL at the 'resonance wavelength', λ_R,

$$\lambda_R = \lambda_0/2\gamma^2(1 + K^2/2),$$

where λ_0 is the magnetic period of the undulator, and γ is the Lorentz factor. γmc^2 is the electron beam energy and $K = eB\lambda_0/2\pi mc$ is the deflection parameter proportional to the magnetic field, B, of the undulator. In our CLIO FEL the wavelength is tuned continuously by varying the undulator gap, which modifies the K parameter. The discrete modification of the electron energy, γmc^2, allows one to change the tuning range.

CLIO is a user facility operating in the mid-IR region, designed to produce a high-performance tunable laser beam. It uses a linear accelerator operated between 20 and 60 MeV, covering a 4–50 μm spectral range. CLIO has specificities which distinguish it from the few other existing FEL facilities in the world. The electron gun has the unique property to deliver pulses whose separation can be adjusted between 32 and 4 ns within the macropulse. The macropulse repetition rate is adjustable between 1 and 50 Hz. Another interesting feature of CLIO is the versatility of the duration of the laser micropulses within the range 0.5–6 ps. This allows the user to choose the laser peak power and the relevant spectral width.

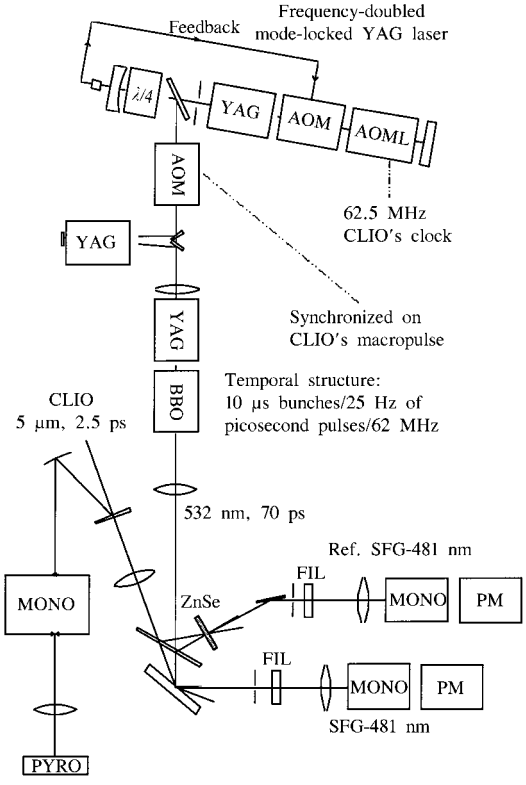

Figure 1
Schematic diagram of the experimental SFG set-up (Peremans *et al.*, 1994). Key: MONO = monochromator; PM = photomultiplier; PYRO = pyrometer; AOM = opto-acoustic modulator; AOML = opto-acoustic mode-locker.

We have synchronized an actively mode-locked Nd:YAG laser to perform a non-linear optical investigation of the vibrational properties and the dynamics of various interfaces, by SFG and DFG (Peremans *et al.*, 1994; Tadjeddine & Peremans, 1998). A schematic diagram of our experimental SFG set-up is shown in Fig. 1.

2.2. *Vibrational spectroscopy of hydrogen–platinum electrochemical interface*

The identification of the adsorbed species is an important step towards a microscopic description of the interface structure and its correlation with the reactivity of electrochemical systems. Since the mean free path of an electron is very small in condensed matter, the photon is the only probe that can be used in the electrochemical environment, which explains the development of IR and surface-enhanced Raman spectroscopies. However, in linear optics the interface contribution to the overall signal is four to five orders of magnitude weaker than that of the bulk electrolyte, which seriously complicates the analysis of IR data. This difficulty has been removed by using the SFG non-linear optical technique, which is inherently interface-sensitive, at the boundary between centrosymmetric media where second-order optical processes are forbidden, within the electric dipole approximation (Shen, 1984; Guyot-Sionnest & Tadjeddine, 1990). We shall discuss in the following the case of hydrogen adsorbed on a platinum single-crystal electrode. Hydrogen is involved as a reactant or product in numerous surface catalyzed reactions. In electrochemistry the hydrogen evolution reaction (HER) is of fundamental interest with regard to the development of efficient and environmentally benign technologies for energy conversion and storage (Parsons & VanderNoot, 1988). The electrochemical deposition of hydrogen on platinum has attracted much interest. At underpotential (positive of the HER onset potential), the deposition of the stable hydrogen monolayer is extensively studied by cyclic voltametry and is found to be sensitive to the surface structure (Clavilier, 1980). At overpotential (negative of the HER onset potential), the kinetics of the HER appear to be insensitive to the surface structure and predict a low coverage of HER intermediate, which contrasts with the underpotential-deposited (UPD) hydrogen coverage that reaches 0.66 monolayer on the positive side of that potential limit. SFG offers the possibility of recording absolute vibrational spectra without the need to make reference to a particular potential. This advantage also allows probing of the interface at overpotential where the perturbation of the electrolyte by the release of H_2 hampers the performance of differential IR and Raman spectroscopies. Moreover, the power of the IR beam provided by CLIO FEL gives the SFG spectrometer enough sensitivity to record the vibrational signature of the hydride interface in the electrochemical environment (Peremans & Tadjeddine, 1994, 1996).

2.2.1. *Underpotential deposition of H on Pt.* The potential-evolved SFG spectra of H–Pt(111), H–Pt(100), H–Pt(110) and H–Pt in 0.1*M* H_2SO_4 solution are shown in Fig. 2. Detailed analysis of the data has been reported by Peremans & Tadjeddine (1994, 1996). The internal structure of the SFG spectra can be resolved into two surface orientation-dependent resonances. Their peak positions are 1890 and 1970 cm^{-1} for Pt(100), 1900 and 1980 cm^{-1} for Pt(110), and 1945 and 2020 cm^{-1} for Pt(111). Only H–Pt vibrations can account for the observed SFG resonances. At underpotential, the frequency range of the H–Pt(*hkl*) SFG resonance (1800–2100 cm^{-1}) indicates that the UPD hydrogen occupies a terminal adsorption site. They are broad and shifted to lower wavenumber in comparison with the terminal H–Pt IR band detected at 2100 cm^{-1} in metallic hydride complexes or on platinum aggregates in the gas phase. This shift and broadening is a consequence of the hydrogen bonding between the adsorbed hydrogen and the water molecules of the electrolyte. This interaction between the hydride interface and the electrolyte double layer may explain the different adsorption behaviour of hydrogen in electrochemical and ultra-high-vacuum environments. In the latter case, its coordination on all metals is always found to be multifold (Christmann, 1988).

2.2.2. *Overpotential deposition of hydrogen on platinum.* The SFG resonances associated with the UPD hydrogen are not perturbed by the new hydrogen adspecies showing up in the overpotential range. This indicates that the UPD hydrogen remains on the surface at a potential negative of the HER onset and that the overpotential deposited (OPD) hydrogen is either coadsorbed with the UPD hydrogen or its coverage remains low such that it may not significantly affect the UPD hydrogen. The frequency of the SFG resonance at 1770 cm^{-1} that appears at overpotential on all the samples lies out of the conventional spectral ranges of the vibrations of multifold (500–1300 cm^{-1}) and onefold (1800–2200 cm^{-1}) coordinated hydrogen–metal bonds. It is, however, close to the H–Pt vibration in hydride complexes of the form H_2Pt–*R* (1735 cm^{-1}), suggesting a dihydride adsorption configuration of the adsorbed intermediate of the hydrogen evolution. This result is the first direct identification of the adsorbed intermediate of the hydrogen evolution reaction.

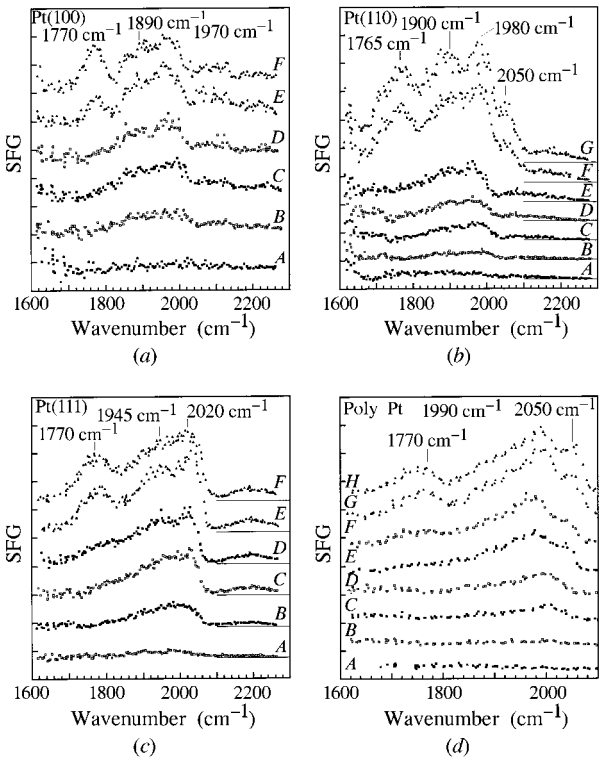

Figure 2
Potential evolved SFG spectra of a platinum electrode in contact with H_2SO_4 0.1*M* electrolyte. Curves are offset on the *y* axis for clarity. Electrode potentials: 0.55 (*A*), 0.45 (*B*), 0.35 (*C*), 0.25 (*D*), 0.5 (*E*), 0.15 (*F*), 0.05 (*G*), −0.05 (*H*) and −0.15 V/NHE (normal hydrogen electrode).

3. Use of the two-colour configuration of CLIO in the study of low-dimensional semiconductor structure

The double undulator of CLIO allows the production of picosecond laser pulses at two different wavelengths, λ_1 and λ_2, simultaneously, in a wavelength range from λ = 5 μm to λ = 18 μm, and with a wavelength separation of the two colours up to $\lambda_1 - \lambda_2$ = 5 μm (Ortéga *et al.*, 1995).

The two-colour configuration has been used recently for the study of stimulated emission in three-level quantum well structures of GaAs–GaAlAs, at 77 K (Gauthier-Lafaye *et al.*, 1997). The low-wavelength beam was set at

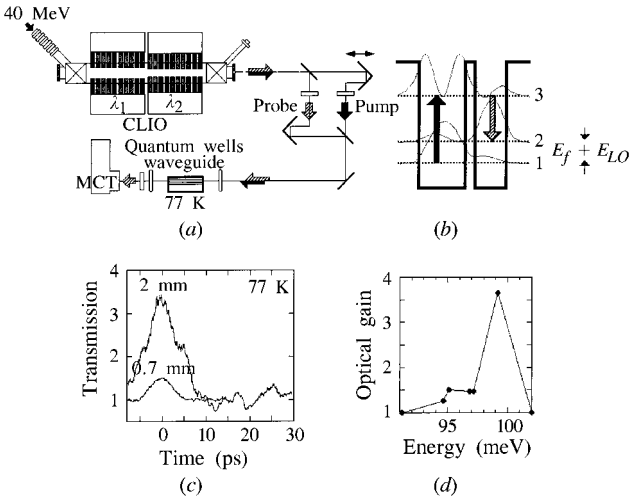

Figure 3
Intersubband stimulated emission pump-probe experiment using a two-colour CLIO FEL (Gauthier *et al.*, 1997). (*a*) Schematic diagram of the experimental set-up. MCT = mercury-cadmium-tellurium. (*b*) Calculated conduction band profile of the asymmetric coupled quantum wells. The arrows indicate the absorption and emission processes. (*c*) Intersubband stimulated gain at 12.5 mm and 77 K, for 0.7 and 2 mm-long waveguide, measured *versus* the time delay between the pump and probe beams at 9.2 and 12.5 μm, respectively. (*d*) Intersubband stimulated gain spectrum as a function of the probe wavelength.

10 mm and acted as an optical pump between the ground and the second excited subband level of the well. The second colour was used as a probe of the stimulated gain and scanned between 12 and 15 mm. Fig. 3 displays the layout of the experiment and the first set of data, showing an optical gain of two to three. Details of the data analysis can be found in the work of Gauthier-Lafaye *et al.* (1997).

4. Resonant two-photon ionization of Xe using a benchtop laser synchronized with a synchrotron radiation pulse

The complementary characteristics of lasers and synchrotron radiation offer new experimental possibilities and some particular advantages when the two light sources are used in combination (Nahon *et al.*, 1996). The main advantage of synchrotron radiation is the very large energy range of the emitted photons and its easy tunability. The combination of lasers and synchrotron radiation for the study of laser-excited atoms was introduced in the early 1980s (for a review, see Wuilleumier *et al.*, 1992). In these experiments a continuous-wave (c.w.) ring dye laser was used to excite the outermost electron of an alkaline atom, while the subsequent photoionization by synchrotron radiation allowed a direct investigation of the correlation effects introduced by the change of the orbit of the outer electron.

For studies of highly excited states and resonant autoionization states, the pump-probe scheme is inverted and synchrotron radiation is used for the pump process. In order to counterbalance the lower excitation rate in the pump process and the shorter lifetime of the excited states, synchronization between the pulses of the mode-locked laser and the synchrotron radiation has to be applied. A detailed description of the technique is given by Lacoursière *et al.* (1994). As an example, we present a study recently performed at the Super-ACO storage ring on the two-photon ionization of Xe atoms *via* the Xe* $5s^2 5p^5 5d$ $[3/2]_1$ resonance (Meyer *et al.*, 1996). A diagram of the pump-probe excitation used for the two-photon excitation of Xe is displayed in Fig. 4. The synchrotron radiation ($h\nu = 10.4$ eV) excites the Xe* $5p^5 5d$ $[3/2]_1$ resonance lying below the first ionization threshold. The linewidth of this resonance is mainly determined by Doppler broadening. The excited atoms are ionized in a second step by the laser

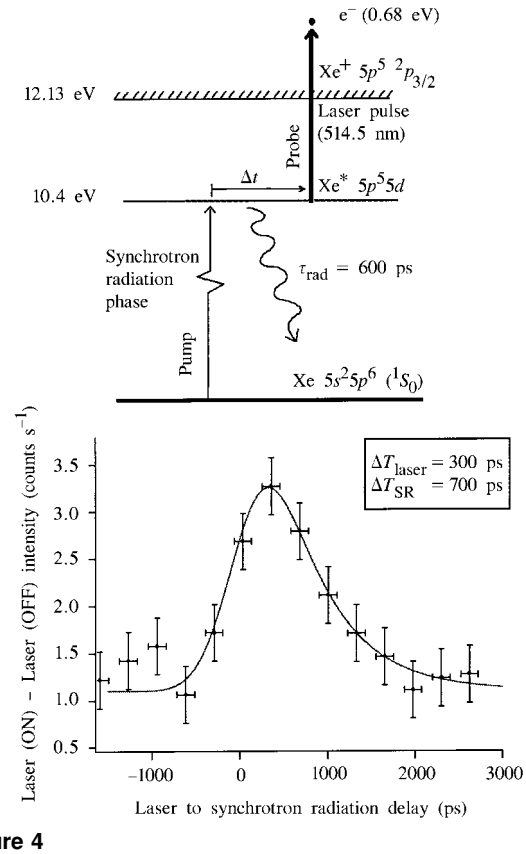

Figure 4
Top: schematic energy diagram illustrating the excitation pathway used to ionize atomic Xe *via* a resonant two-photon process. Bottom: two-photon ionization signal of Xe as a function of the delay between the laser and the synchrotron radiation pulses (Meyer *et al.*, 1996).

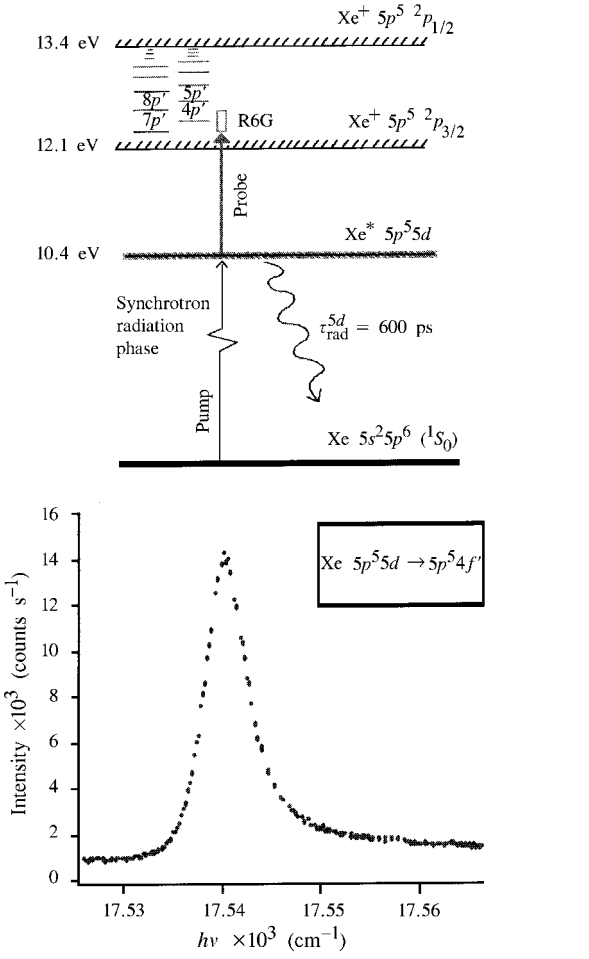

Figure 5
Top: schematic diagram of the excitation pathway used to ionize atomic Xe *via* a double-resonance two-photon process. Bottom: two-photon ionization signal of Xe as a function of the wavelength ionizing laser (Gisselbrecht *et al.*, 1997).

pulse (514 nm line of the Ar^+ laser) if the two light pulses are both present in the interaction region within a short time window determined by the lifetime of the Xe* $5p^5 5d$ state (Γ = 600 ps). By changing the delay between the synchrotron radiation and the laser pulses, the decreasing population of the excited state and the corresponding lifetime can be determined. The lower part of Fig. 4 displays the resulting ionization signal as a function of the delay between the two light pulses. Simulation reproduces the experimental data points and demonstrates that we are able to synchronize and to control on a nanosecond timescale the pulses of a mode-locked Ar^+ laser with respect to the synchrotron radiation pulses of the Super-ACO storage ring.

The wavelength of the ionizing laser (linear dye laser in synchronous pumping) was then scanned within the energy range accessible with Rhodamine 6G to study the Xe* $5p^5 4f'$ autoionization resonance (Gisselbrecht *et al.*, 1997). The observed ionization signal as a function of the laser wavelength is given in Fig. 5, together with the corresponding schematic energy diagram. The obtained asymmetric line profile is characteristic of an autoionizing resonance and can be described by the formalism developed by Fano. The determination of the line profile parameters (linewidth, asymmetric resonant and non-resonant ionization cross section) provides a detailed basis for comparison with theories treating the complicated electronic interaction of a multi-electron atom

5. Surface states and space charge layer dynamics on Si(111) 2 × 1: an FEL–synchrotron radiation study (Marsi *et al.*, 1997)

Studies of non-equilibrium conditions in semiconductors are usually performed by optically generated electron–hole pairs using photons with energies greater than the band gap. The photoexcited carriers are separated by the pre-existing band-bending electric field, producing a surface photovoltage (SPV) which flattens the energy bands, until recombination processes (both at the surface and in the bulk) lead the system back to equilibrium conditions. However, no direct bending-band variations related to surface carrier dynamics in the transient regime have been observed.

A novel approach to two-photon spectroscopy, based on the combined use of a naturally synchronized storage ring FEL and of synchrotron radiation, has been recently performed at LURE. It is then possible to perform a time-resolved core-level photoemission study with the synchrotron radiation on FEL-photoexcited cleaved Si(111) 2 × 1 surfaces with sub-nanosecond temporal resolution and high surface sensitivity, and directly observe how surface states affect the dynamics of the transient space charge layer.

Experiments were performed on Super-ACO at LURE, Orsay, using a two-colour pump-probe approach, where the Super-ACO storage ring FEL acted as a pump to photoexcite carriers, and synchrotron radiation core-level photoemission was used to follow the band-bending by measuring the Si 2*p* core-level binding-energy variations.

Fig. 6 illustrates the experimental procedure followed to determine the band-bending dynamics: the SPV was measured, for a given time delay between the FEL and synchrotron radiation pulses, by the shift of the Si 2*p* core level taken on the FEL photoexcited surface with respect to the one at electrostatic equilibrium, taken as reference.

Fig. 7 presents the time-dependence of the transient SPV for three different surfaces: (*a*) corresponds to a good cleave, (*b*) to a surface where part of the 2 × 1 reconstruction was destroyed by contamination-induced defects, and (*c*) to one where almost no evidence of reconstruction was left.

These results were explained by the specific properties of the Si(111) 2 × 1 surface electronic structure, which is characterized by a filled *p*-bonding chain, and an empty

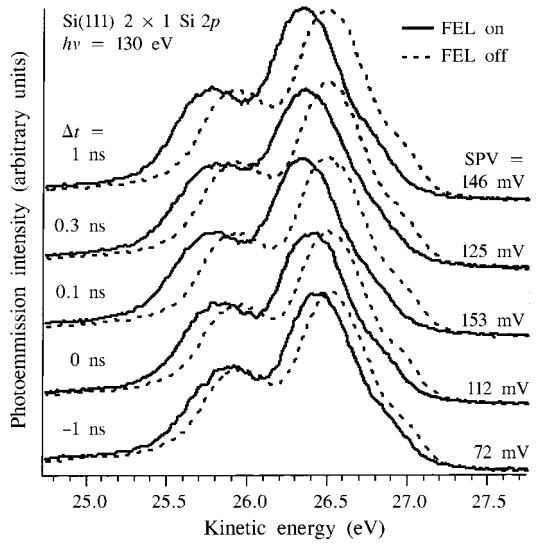

Figure 6
Si 2*p* core-level spectra of Si(111) 2 × 1 for various time delays between the UV FEL pump and the synchrotron radiation probe.

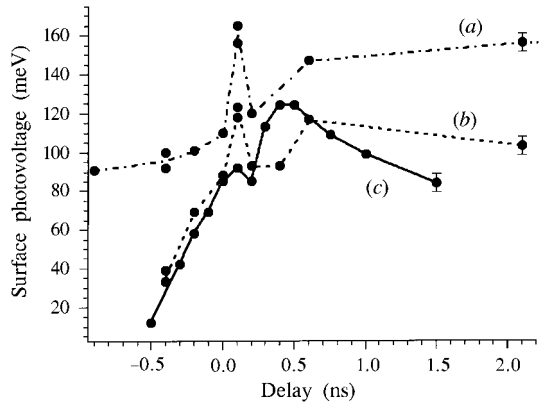

Figure 7
Surface photovoltage *versus* time delay between FEL and synchrotron radiation pulses for different Si(111) surfaces: (*a*) high-quality 2 × 1 reconstructed surface, (*b*) partially contaminated and (*c*) with strong contamination-induced defects.

π^*-antibonding chain, separated by a surface band gap of 0.45 eV. The p state lies very close to the valence band maximum; π^* is responsible for pinning the Fermi level and determining the equilibrium band bending. The existence of the dip in the SPV decay curve, related to the presence of the 2×1 reconstruction, can be related to the charge flow to and from these surface states. In particular, a key point in interpreting the data is that the hole exchange between the p state and the valence band maximum is about 1000 times faster than the electron exchange between π^* and the conduction band minimum. The presence of defects disrupts this charge flow mechanism and increases the coupling between surface and bulk, making the overall recombination process faster.

6. Conclusions

The combination of complementary photon sources appears to be a very effective and very powerful tool for the investigation of different systems. We have shown that the high power and the picosecond pulse duration of the mid-IR CLIO FEL makes this laser well adapted for investigation of the non-linear optical properties of surfaces and interfaces. In particular, the synchronization of a YAG benchtop laser to the temporal structure of CLIO allowed us to perform visible–IR SFG and DFG and to probe selectively the vibrational and the dynamics of buried surfaces such as the electrochemical interface. Using the two-colour configuration of CLIO, which provides two synchronized tunable IR beams, it is possible to perform a time-resolved pump-probe study of the intersubband stimulated emission of asymmetric quantum wells.

The different, partly complementary, characteristics of lasers and synchrotron radiation offer new experimental possibilities and some particular advantages when the two light sources are used in combination. The main advantage of synchrotron radiation is the very large energy range of the emitted photons and its easy tunability, while lasers are known for their high flux and temporal and spatial resolution. Studies of photoexcitation and photoionization in different subshells of many atoms and molecules have been performed during recent years. We have shown, as an example, the use of the combination of laser and synchrotron radiation to investigate in a pump-probe arrangement the ionization of Xe atoms *via* the resonant state Xe* $5p^5 5d\ [3/2]_1$.

Finally, the use of the naturally synchronized UV storage ring FEL and synchrotron radiation allows the direct study of the dynamics of surface states and space charge layer on semiconductor surfaces and interfaces, using time-resolved core-level spectroscopy.

AT is greatly indebted to Dr Irène Nenner, CEA-DSM: DRECAM (Saclay, France) for her kind and fruitful discussions in preparing this contribution.

References

Christmann, K. (1988). *Surf. Sci. Rep.* **9**, 1–89.
Clavilier, J. (1980). *J. Electroanal. Chem.* **107**, 211–216.
Gauthier-Lafaye, O., Sauvage, S., Boucaud, B., Julien, F. H., Prazeres, R., Glotin, F., Ortéga, J. M., Thierry-Mieg, V., Planel, R. & Leburton, J. P. (1997). *Appl. Phys. Lett.* **70**, 3197–3199.
Gisselbrecht, M., Marquette, A. & Meyer, M. (1997). To be published.
Guyot-Sionnest, P. & Tadjeddine, A. (1990). *Chem. Phys. Lett.* **172**, 341–347.
Lacoursière, J., Meyer, M., Nahon, L., Morin, P. & Larzillière, M. (1994). *Nucl. Instrum. Methods Phys. Res. A*, **351**, 545–553.
Marsi, M., Couprie, M. E., Nahon, L., Garzella, D., Hara, T., Bakker, R., Billardon, M., Delboublé, A., Indlekofer, G. & Taleb-Ibrahimi, A. (1997). *Appl. Phys. Lett.* **70**, 895–897.
Meyer, M., Nahon, L., Lacoursière, J., Gisselbrecht, M., Morin, P. & Larzillière, M. (1996). *J. Electron Spectrosc. Relat. Phenom.* **79**, 343–346.
Nahon, L., Meyer, M., Lacoursière, J., Gisselbrecht, M., Morin, P. & Larzillière, M. (1996). *Frontiers Sciences Series Atomic and Molecular Photoionization*, edited by A. Yagishita & T. Sasaki, pp. 1–10. Tokyo: Universal Academic Press.
Ortéga, J. M. (1996). *Synchrotron Rad. News*, **9**, 20–33.
Ortéga, J. M., Prazeres, R., Glotin, F. & Jaroszinski, D. (1995). *Phys. Rev. Lett.* **74**, 2224–2228.
Parsons, R. & VanderNoot, T. (1988). *J. Electroanal. Chem.* **229**, 9–30.
Peremans, A., Guyot-Sionnest, P., Tadjeddine, A., Glotin, F., Ortéga, J. M. & Prazeres, R. (1994). *Nucl. Instrum. Methods Phys. Res. A*, **331**, 146–147.
Peremans, A. & Tadjeddine, A. (1994). *Phys. Rev. Lett.* **73**, 3010–3014.
Peremans, A. & Tadjeddine, A. (1996). *J. Chem. Phys.* **103**, 7197–7203.
Shen, Y. R. (1984). *The Principles of Non-Linear Optics.* New York: Wiley-Interscience.
Tadjeddine, A. & Peremans, A. (1998). *Spectroscopy for Surface Science*, edited by R. J. H. Clark & R. E. Hester, pp. 159–217. London: John Wiley.
Wuilleumier, F. J., Cubaynes, D. & Bizau, J. M. (1992). *Ann. Phys.* **17**(C1), 197–217.